On the Digital Control of MEMS Gyroscopes: a Robust Approach

Fabricio Saggin, Cécile Pernin, Anton Korniienko, Gérard Scorletti, Christophe Le Blanc

On the Digital Control of MEMS Gyroscopes: a Robust Approach

Fabrício Saggin*, Cécile Pernin*, Anton Korniienko*, Gérard Scorletti* and Christophe Le Blanc†
* Laboratoire Ampère, Ecole Centrale de Lyon, Université de Lyon, France
† Asygn, Grenoble, France

I. Abstract

This document provides further details on the paper "Digital Control of MEMS Gyroscopes: a Robust Approach" [1]. These details concern the choice of the weighting functions for the H_∞ synthesis.

II. System Description and Control Objectives

As described in [1], the object of study is the control of a MEMS gyroscope.

The considered control architecture is represented in Fig. 1, where G_c is the model of the gyroscope with actuation and instrumentation, and K_c is the controller. Both are Multi Input Multi Output (MIMO) systems, in continuous time (CT). The controller K_c directly applies a signal u_x (resp. u_y) on the drive (resp. sense) mode. The signal d_x (resp. d_y) is the disturbance on u_x (resp. u_y) and represents the Coriolis force acting on the drive (resp. sense) mode. Thus, estimating d_y allows to compute the Coriolis force, and then the angular rate. The input signals of G_c are u_{d_x} and u_{d_y}. The outputs of G_c are the signals x and y, representing voltages proportional respectively to the displacements on the drive mode and on the sense mode. The measurement noise is denoted n_x (resp. n_y) on the drive (resp. sense) mode. The resonance frequency (in $\mathrm{rad/s}$) of the drive (resp. sense) mode is denoted ω_{0_x} (resp. ω_{0_y}).

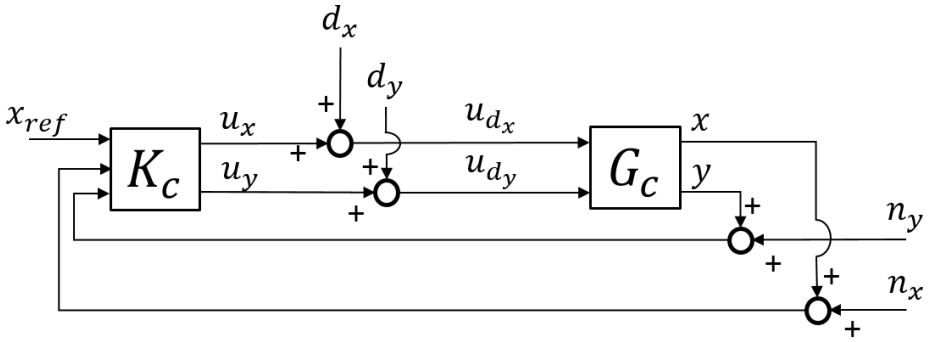

Fig. 1: Control architecture.

A discrete-time (DT) model of the gyroscope is obtained by identification and the electrical coupling is compensated, as described in [2], [3]. From the DT model, a CT model G_c is obtained by using the bilinear (or Tustin) transform. A controller K_c is calculated from G_c. The frequency distortion induced by the bilinear transform is compensated when the bilinear transform is applied to K_c, obtaining a DT controller K_d.

The Bode diagram of the gyroscope G_c is presented in Fig. 2 and G_c is partitioned as follows:

$$G_c(s) = \begin{bmatrix} G_{c_{xx}}(s) & G_{cxy}(s) \\ G_{c_{yx}}(s) & G_{c_{yy}}(s) \end{bmatrix}, \tag{1}$$

where the main dynamic of $G_{c_{xx}}$ (resp. $G_{c_{yy}}$) corresponds to a resonator with resonance frequency ω_{0_x} (resp. ω_{0_y}) and quality factor Q_x (resp. Q_y).The transfers $G_{c_{xy}}$ and $G_{c_{yx}}$ model the couplings between drive and sense modes. The transfer $G_{c_{yx}}$ presents resonance peaks at ω_{0_x} and ω_{0_y} and a magnitude that is globally smaller than that of $G_{c_{xx}}$ and $G_{c_{yy}}$. The transfer $G_{c_{xy}}$ is negligible for the MEMS sensor used in this study. Finally, the actuation and instrumentation circuitry justifies the phase of the transfers.

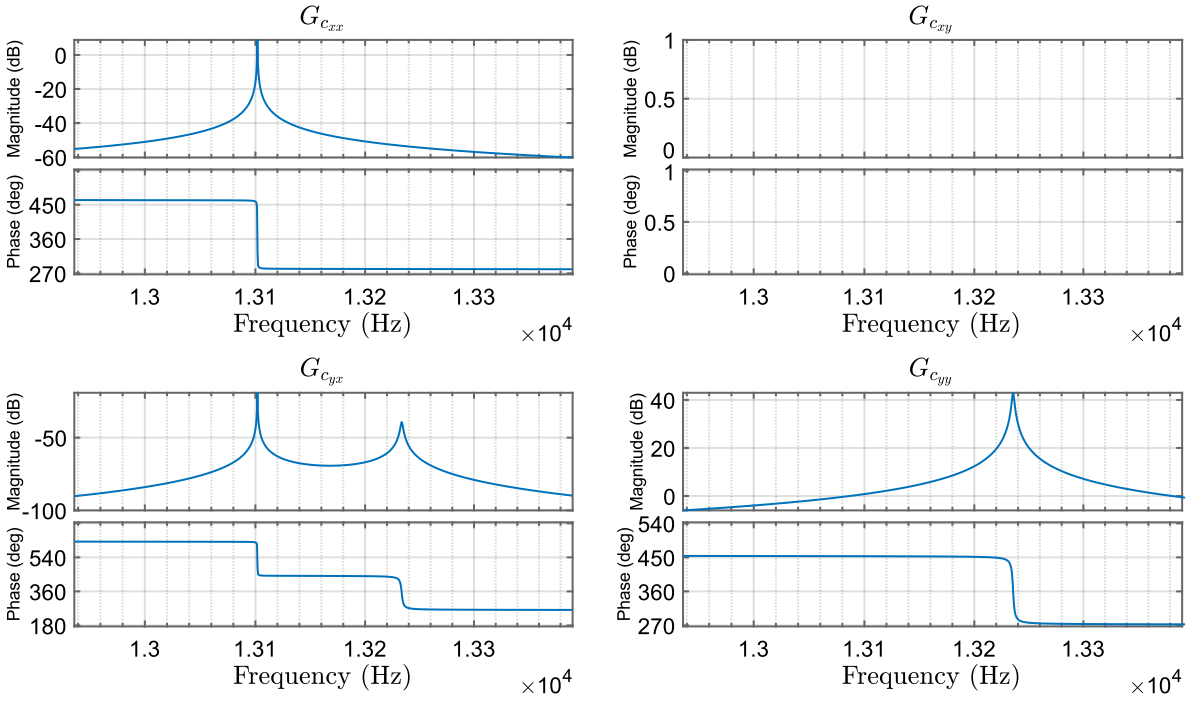

Fig. 2: Bode diagram of the gyroscope model.

The main control specifications are :

1) Track the sinusoidal reference signal $x_{ref}(t) = A_{ref} \sin(\omega_{0_x} t)$ with an error $\varepsilon_x(t) = x_{ref}(t) - x(t)$, such that $|\varepsilon_x| < \varepsilon_{x_{max}} |A_{ref}|$ in steady-state, where $A_{ref} \in \mathbb{R}$ and $\varepsilon_{x_{max}} \in \mathbb{R}^+$.
2) Reject the disturbance $d_y(t) = A_{d_y} \sin(\omega_{0_x} t + \phi_y)$ on the signal u_{d_y}, *i.e.*, with a maximum error u_{d_y} such that $|u_{d_y}| < \varepsilon_{u_{max}} |A_{d_y}|$, where $A_{d_y} \in \mathbb{R}$, $\phi_y \in \mathbb{R}$ and $\varepsilon_{u_{max}} \in \mathbb{R}^+$.
3) Robust stability against model uncertainties in low and high frequencies.

Secondary control objectives are also considered:

- Minimize the control effort u_x on the drive mode.
- Limit the influence of the measurement noises n_x and n_y.
- Reject the disturbance $d_x(t) = A_{d_x} \sin(\omega_{0_x} t + \phi_x)$ with an error $\varepsilon'_x(t) = x(t)$, such that $|\varepsilon'_x| < \varepsilon'_{x_{max}} |A_{d_x}|$ in steady-state, where $A_{d_x} \in \mathbb{R}$, $\phi_x \in \mathbb{R}$ and $\varepsilon'_{x_{max}} \in \mathbb{R}^+$.

III. Choice of the weighting function parameters

In the H_∞ synthesis, the controller design is formulated as an optimization problem subject to mathematical constraints, which express performance and stability robustness requirements into a mathematical criterion to be minimized. The choice of the input and output signals and of the weighting functions, *i.e.*, the so-called H_∞ criterion, must be adapted to the specifications.

We consider the criterion presented in Fig. 3, where the signals of interest $\widetilde{w} = (x_{ref},\, d_x,\, d_y,\, n_x,\, n_y)^T$ and $\widetilde{z} = (\varepsilon_x,\, u_x,\, u_{d_y})^T$, weighting functions $W_w = \mathrm{diag}\,(W_{w_1}, \ldots W_{w_5})$ and $W_z = \mathrm{diag}\,(W_{z_1}, \ldots W_{z_3})$ are defined with $w = (w_1, w_2, w_3, w_4, w_5)^T = W_w^{-1} \widetilde{w}$ and $z = (z_1, z_2, z_3)^T = W_z \widetilde{z}$.

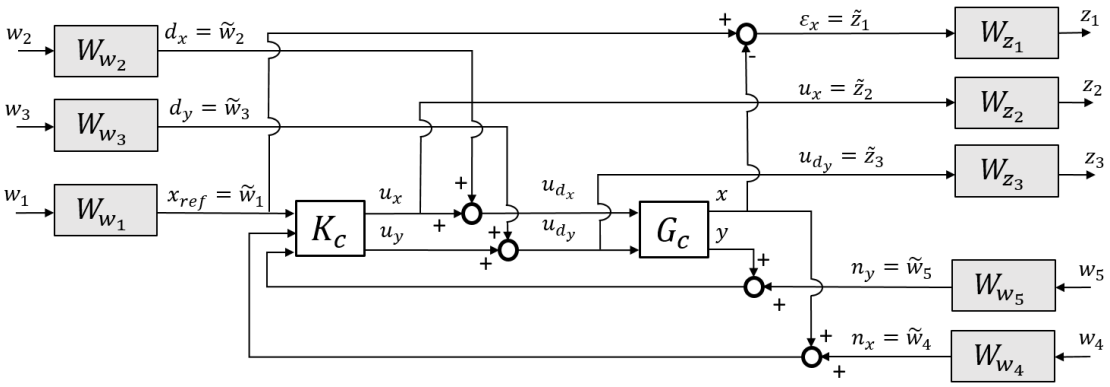

Fig. 3: H_∞ criterion.

The H_∞ problem is the following: for a given γ, find a controller such that the weighted closed-loop transfer functions are stable and

$$\left\| \begin{bmatrix} T_{w_1 \to z_1} & T_{w_2 \to z_1} & T_{w_3 \to z_1} & T_{w_4 \to z_1} & T_{w_5 \to z_1} \\ T_{w_1 \to z_2} & T_{w_2 \to z_2} & T_{w_3 \to z_2} & T_{w_4 \to z_2} & T_{w_5 \to z_2} \\ T_{w_1 \to z_3} & T_{w_2 \to z_3} & T_{w_3 \to z_3} & T_{w_4 \to z_3} & T_{w_5 \to z_3} \end{bmatrix} \right\|_\infty < \gamma, \tag{2}$$

where we use the notation $T_{a \to b}$ to denote the transfer from a signal a to a signal b.

If the above problem has a solution with $\gamma < 1$, then it can be shown (see [4]) that (2) implies

$$\forall \omega \in \mathbb{R},\ \forall k \in \{1, ..., 5\}, \forall\, l \in \{1, ..., 3\},\ |T_{\tilde{w}_k \to \tilde{z}_l}(j\omega)| < |W_{w_k}(j\omega) W_{z_l}(j\omega)|^{-1}. \tag{3}$$

Therefore, the choice of the weighting functions allows to impose upper bounds on the magnitude of the closed-loop transfer functions and thus to ensure compliance with the specifications, which are themselves expressed as upper bounds.

Two main types of dynamic weighting functions are used in this work, which are adapted to the reference tracking and disturbance rejection of sinusoidal signals [5]:

1) An "amplification" weighting function W_{amp}

$$W_{amp}(k, W_{max}, W_{int}, \omega_{min}, \omega_{max}, s) = k \cdot \frac{s^2 + \alpha s + \omega_{min}\omega_{max}}{s^2 + \alpha / W_{max} \cdot s + \omega_{min}\omega_{max}} \tag{4}$$

with

$$\alpha = (\omega_{max} - \omega_{min}) \cdot W_{max} \cdot \sqrt{\frac{W_{int}^2 - 1}{W_{max}^2 - W_{int}^2}}, \tag{5}$$

where $k > 0$, $W_{max} > W_{int} > 0$ and $\omega_{max} > \omega_{min} > 0$ can be chosen by the user.
The magnitude plot of this type of weighting function is given in Fig. 4, with $\omega_0^2 = \omega_{min} \cdot \omega_{max}$.

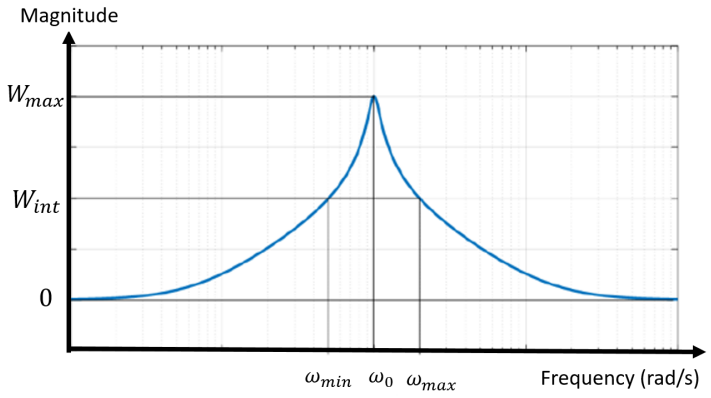

Fig. 4: Magnitude plot of W_{amp}/k.

2) An "attenuation" weighting function W_{att}

$$W_{att}(k, W_{min}, W_{int}, \omega_{min}, \omega_{max}, s) = k \cdot \frac{s^2 + \beta W_{min} s + \omega_{min}\omega_{max}}{s^2 + \beta s + \omega_{min}\omega_{max}} \tag{6}$$

with

$$\beta = (\omega_{max} - \omega_{min}) \cdot \sqrt{\frac{1 - W_{int}^2}{W_{int}^2 - W_{min}^2}} \tag{7}$$

The magnitude of this transfer is given in Fig. 5, with $\omega_0^2 = \omega_{min} \cdot \omega_{max}$.

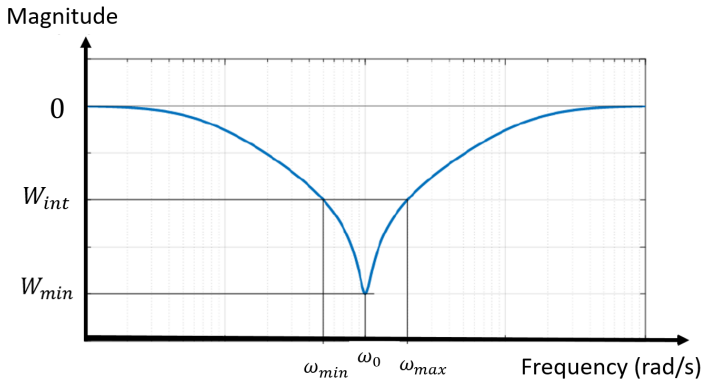

Fig. 5: Magnitude plot of W_{att}/k.

The desired specifications can be expressed through the choice of the weighting functions and their parameters, as follows.

Main Control Specifications

- *Reference tracking:*
  The signals of interest are x_{ref}, the reference signal, and ε_x, the tracking error to be minimized. The function to be worked on is $T_{x_{ref} \to \varepsilon_x}$. The objective is to track a sinusoidal reference signal x_{ref} of frequency ω_{0_x}. More precisely, the first control specification demands:

$$\left| T_{x_{ref} \to \varepsilon_x}(j\omega_{0_x}) \right| < \varepsilon_{x_{max}} \tag{8}$$

  For $k = l = 1$, (3) is equivalent to

$$\forall \omega \in \mathbb{R},\ \left| T_{x_{ref} \to \varepsilon_x}(j\omega) \right| < \left| W_{z_1}(j\omega) W_{w_1}(j\omega) \right|^{-1}. \tag{9}$$

Thus, (8) can be enforced using (9) via the product $W_{z_1}W_{w_1}$. The weighting functions must be chosen so that $|W_{w_1}(j\omega_{0_x})W_{z_1}(j\omega_{0_x})|^{-1} \leq \varepsilon_{x_{max}}$.
The weighting functions are selected such that:

$$W_{w_1} \cdot W_{z_1} = W_{amp}(k_1, W_{max_1}, W_{int_1}, \omega_{min_1}, \omega_{max_1}) \tag{10}$$

with

$$\begin{cases} \omega_{max_1} = \omega_{0_x} + \delta\omega_x \\ \omega_{min_1} = \omega_{0_x} - \delta\omega_x \\ W_{int_1} = \frac{1}{\varepsilon_{x_{max}} \cdot k_1} \end{cases}, \tag{11}$$

where $\delta\omega_x > 0$ is associated with the reference tracking bandwidth, $k_1 > 0$ and $W_{max_1} > 0$. In general, these last parameters are chosen by the user iteratively.

- *Disturbance rejection on the sense mode:*
The signals of interest are d_y, the disturbance, and u_{d_y}, the estimation error to be minimized. The function to be worked on is $T_{d_y \to u_{d_y}}$. The second control specification demands:

$$\left| T_{d_y \to u_{d_y}}(j\omega_{0_x}) \right| < \varepsilon_{u_{max}} \tag{12}$$

With $k = l = 3$, (3) is equivalent to

$$\forall \omega \in \mathbb{R},\ \left| T_{d_y \to u_{d_y}}(j\omega) \right| < |W_{w_3}(j\omega)W_{z_3}(j\omega)|^{-1}. \tag{13}$$

Similar to the reference tracking, the weighting functions are such that:

$$W_{w_3} \cdot W_{z_3} = W_{amp}(k_2, W_{max_2}, W_{int_2}, \omega_{min_2}, \omega_{max_2}) \tag{14}$$

with

$$\begin{cases} \omega_{max_1} = \omega_{0_x} + \delta\omega_y \\ \omega_{min_1} = \omega_{0_x} - \delta\omega_y \\ W_{int_2} = \frac{1}{\varepsilon_{u_{max}} \cdot k_2} \end{cases}, \tag{15}$$

where $\delta\omega_y > 0$ is associated with the bandwidth of the disturbance rejection on the sense mode, $k_2 > 0$ and $W_{max_2} > 0$. In general, these last parameters are chosen by the user iteratively.

- *Robustness against model uncertainties:*
The identification experiment also provides the model uncertainties related to the drive and sense modes [3]. In general, due to the band-pass characteristic of these resonant modes, the identified model is accurate for the frequencies close to the resonance frequencies, while it is rather uncertain in low and high frequencies.
Qualitatively, to ensure the robust stability of the system against this type of uncertainty, the transfers from n_x and n_y to u_x and u_{d_y} must present the following property: the magnitude is small in the frequency range where the uncertainties are important; and the magnitude can be important where the uncertainties are small [4]. Therefore, the corresponding weighting functions have to present high gains in low and high frequencies, and small gains around the resonance frequencies, similar to attenuation function.

Secondary Control Specifications

- *Minimization of the control effort on the drive mode.*
The signal of interest is u_x. All the transfer functions which have u_x as output signal are considered, but here, we focus on $T_{x_{ref} \to u_x}$, corresponding to the control effort to track the sinusoidal reference on the drive mode. Equation (3) implies that

$$\forall \omega \in \mathbb{R},\ \left| T_{x_{ref} \to u_x}(j\omega) \right| < |W_{w_1}(j\omega)W_{z_2}(j\omega)|^{-1} \tag{16}$$

The gain of $T_{x_{ref}\rightarrow u_x}(j\omega)$ at ω_{0_x} is constrained by the specification of tracking, (*i.e.*, the value of $\varepsilon_{x_{max}}$) and the gains of the gyroscope at ω_{0_x}: $T_{x_{ref}\rightarrow u_x}(j\omega_{0_x})$ cannot be lowered under a minimal value, necessary to ensure the desired reference tracking performance. Consequently, the control effort can only be influenced to a limited extent in steady state. This reasoning is actually valid not only at ω_{0_x}, but also on all the bandwidth $\delta\omega_x$ associated with reference tracking.
However, it is possible to limit the control effort in transient state by minimizing as much as possible the gain of $T_{x_{ref}\rightarrow u_x}(j\omega)$ outside the bandwidth $[\omega_{0_x} - \delta\omega_x; \omega_{0_x} + \delta\omega_x]$. This also enforces the robust stability [4]. The weighting functions are chosen so that $W_{w_1} \cdot W_{z_2}$ behaves like an attenuation function, that is, with low gains around ω_{0_x} and high gains in low and high frequencies.

- *Limit the influence of the measurement noises n_x and n_y*
  The signals of interests are n_x and n_y. The weighting functions are designed to minimize the magnitude of the transfer functions that have n_x and n_y as inputs, for all frequencies. However, similarly to the control effort minimization, trade-offs have to be made between the desired reference tracking and disturbance rejection performances on the one hand, and the noise attenuation on the other hand. Consequently, the weighting functions related to the signals n_x and n_y are chosen so that the transfer functions having n_x and n_y as inputs behave like attenuation functions, that is, with low gains around ω_{0_x} and high gains in low and high frequencies.

- *Disturbance rejection on the drive mode*
  The disturbance d_x represents the Coriolis force acting on the drive mode. The reasoning is the same as for the disturbance rejection on the sense mode, and the weighting functions can be chosen as:

$$W_{w_2} \cdot W_{z_1} = W_{amp}(k_3, W_{max_3}, W_{int_3}, \omega_{min_3}, \omega_{max_3}) \tag{17}$$

  with

$$\begin{cases} \omega_{max_3} = \omega_{0_x} + \delta\omega'_x \\ \omega_{min_3} = \omega_{0_x} - \delta\omega'_x \\ W_{int_3} = \frac{1}{\varepsilon'_{x_{max}} \cdot k_3} \end{cases}, \tag{18}$$

  where $\delta\omega'_x > 0$ is associated with the bandwidth of the disturbance rejection on the drive mode, $\varepsilon'_{x_{max}}$ corresponds to the disturbance rejection error, $k_3 > 0$ and $W_{max_1} > 0$. In general, these last parameters are chosen by the user iteratively.

The final choice of the weighting functions is made keeping in mind that the more important the total order of the weighting functions is, the more important the order of the controller is.

The following numerical values are selected:

$$\begin{cases} \varepsilon_{x_{max}} = 0.005 \\ \delta\omega_x = 2\,\mathrm{rad/s} \\ \varepsilon_{u_{max}} = 0.01 \\ \delta\omega_y = 7\,\mathrm{rad/s} \\ \varepsilon'_{x_{max}} = 0.005 \\ \delta\omega'_x = 2\,\mathrm{rad/s} \end{cases} \tag{19}$$

The selected weighting functions are the following:

$$\begin{cases} W_{w_1} = W_{amp}(k_1, W_{max_1}, W_{int_1}, \omega_{min_1}, \omega_{max_1}) \\ W_{w_2} = W_{amp}(k_3, W_{max_3}, W_{int_3}, \omega_{min_3}, \omega_{max_3}) \\ W_{w_3} = W_{amp}(k_2, W_{max_2}, W_{int_2}, \omega_{min_2}, \omega_{max_2}) \\ W_{z_1} = 1 \\ W_{z_2} = W_{att}(k_4, W_{min_4}, W_{int_4}, \omega_{min_4}, \omega_{max_4}) \\ W_{z_3} = 1 \\ W_{z_4} = W_{att}(k_5, W_{min_5}, W_{int_5}, \omega_{min_5}, \omega_{max_5}) \\ W_{z_5} = W_{att}(k_6, W_{min_6}, W_{int_6}, \omega_{min_6}, \omega_{max_6}) \end{cases} \tag{20}$$

All the parameters of these functions are given in Table I.

TABLE I: Numerical values of the parameters of the weighting functions

k_1	k_2	k_3	k_4	k_5	k_6
$10^{-8/20}$	$10^{-8/20}$	$10^{-8/20}$	$10^{40/20}$	$10^{80/20}$	$10^{40/20}$
W_{int_1}	W_{int_2}	W_{int_3}	W_{int_4}	W_{int_5}	W_{int_6}
$1/(\varepsilon_{x_{max}} \cdot k_1)$	$1/(\varepsilon_{u_{max}} \cdot k_2)$	$1/(\varepsilon'_{x_{max}} \cdot k_3)$	0.001	0.0178	0.224
W_{max_1}	W_{max_2}	W_{max_3}	W_{min_4}	W_{min_5}	W_{min_6}
$4 \cdot W_{int_1}$	$5 \cdot W_{int_2}$	$4 \cdot W_{int_3}$	10^{-5}	$5.6234 \cdot 10^{-5}$	$10^{40/20}$
ω_{min_1}	ω_{min_2}	ω_{min_3}	ω_{min_4}	ω_{min_5}	ω_{min_6}
$\omega_{0_x} - \delta\omega_x$	$\omega_{0_x} - \delta\omega_y$	$\omega_{0_x} - \delta\omega'_x$	0.6	0.75	0.9
ω_{max_1}	ω_{max_2}	ω_{max_3}	ω_{max_4}	ω_{max_5}	ω_{max_6}
$\omega_{0_x} + \delta\omega_x$	$\omega_{0_x} + \delta\omega_y$	$\omega_{0_x} + \delta\omega'_x$	1.6667	1.333	1.111

IV. Synthesis results

In this work, the *Robust Control Toolbox* of Matlab® [6] is used to solve the H_∞ control problem.

With the model G_c and the weighting functions of the previous section, the H_∞ problem (see (2)) is solved with $\gamma = 0.95$. The closed-loop transfer functions are presented in Fig. 8 and Fig. 9. The upper bounds imposed by the weighting functions are respected.

The magnitude of $T_{x_{ref} \to \varepsilon_x}$ is low at the resonance frequency ω_{0_x}: -68 dB, *i.e.*, $4.10^{-4} < \varepsilon_{x_{max}}$. Then, the tracking specification is respected.

The magnitude of $T_{d_x \to \varepsilon_x}$ is low at the resonance frequency ω_{0_x}: -50 dB, *i.e.*, $3.10^{-3} < \varepsilon'_{x_{max}}$. Then, the disturbance rejection specification on the drive mode is respected.

The magnitude of $T_{d_y \to u_{d_y}}$ is low at the resonance frequency ω_{0_x}: -55 dB, *i.e.*, $2.10^{-3} < \varepsilon_{u_{max}}$. Then, the disturbance rejection specification on the sense mode is respected.

The magnitude of the transfers with the noises n_x and n_y as inputs is minimized in low and high frequencies, limiting the influence of the measurement noises on the signals of interest and enhancing the robustness of the system against model uncertainties in these frequency ranges.

The Bode plot of the obtained controller K_c is represented in Fig. 6 and Fig. 7. It is reminded that $In(1)$, or $Input(1)$, is x_{ref}; $In(2)$ is x; $In(3)$ is y; $Out(1)$ is u_x; $Out(2)$ is u_y. The controller has important gains around the resonance frequency ω_{0_x}, which enables to ensure a good tracking of x_{ref} and a good estimation of d_y. Its gains are weak in low and high frequencies, which enables to minimize the control effort in transient state, to limit the influence of the measurement noise on the signals of interest and to enhance robustness.

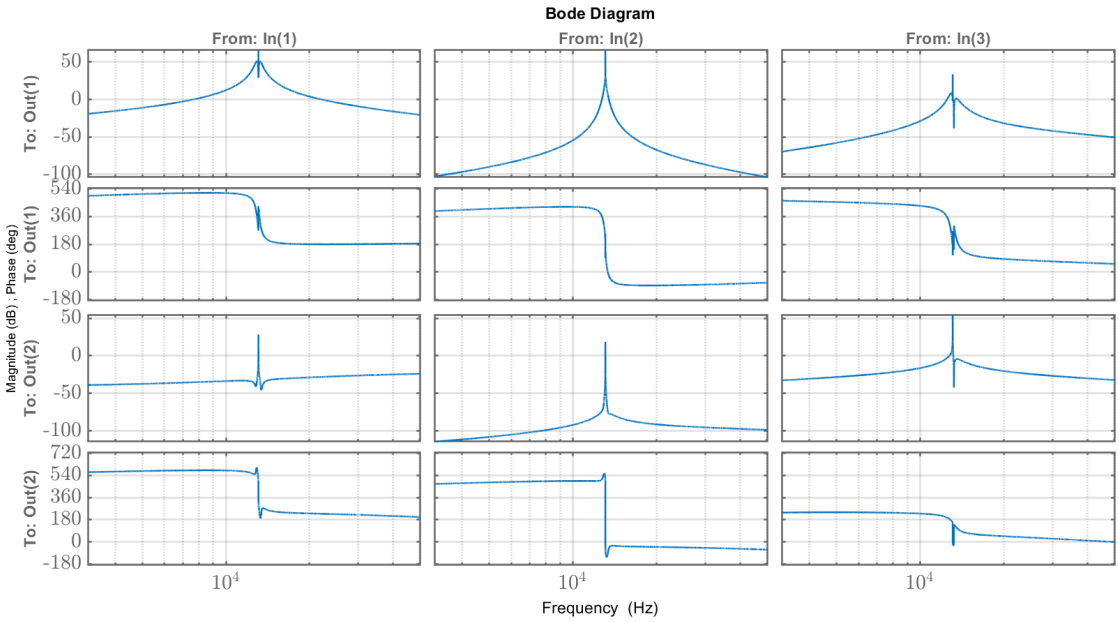

Fig. 6: Bode plot of K_c.

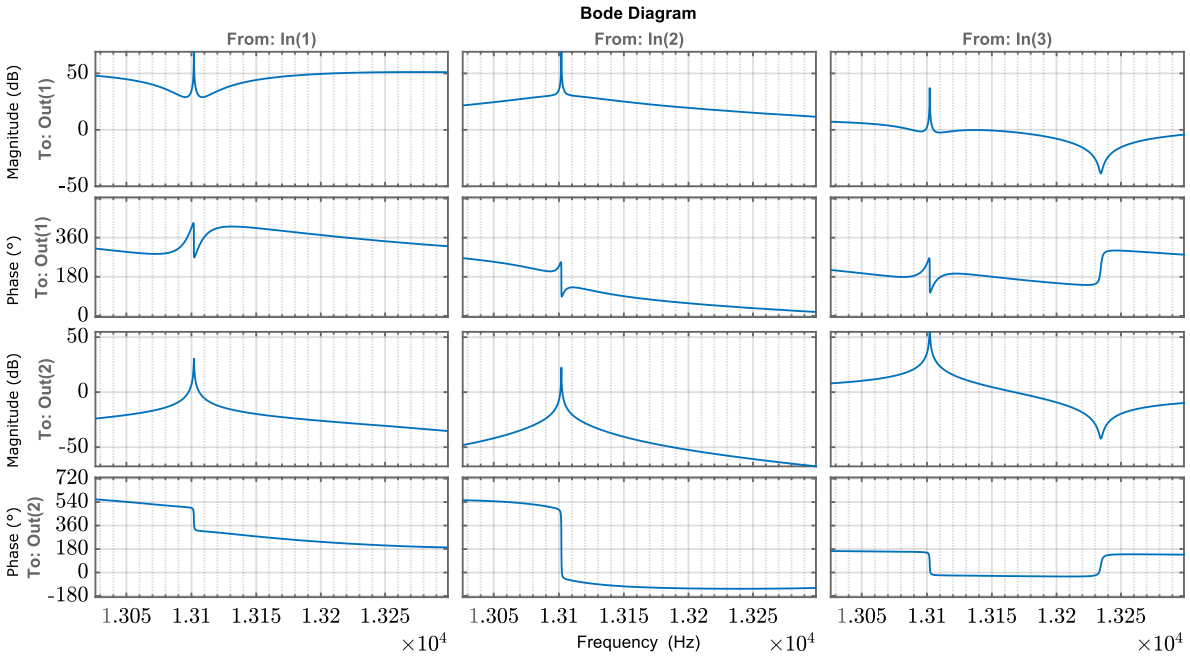

Fig. 7: Bode plot of K_c – zoom.

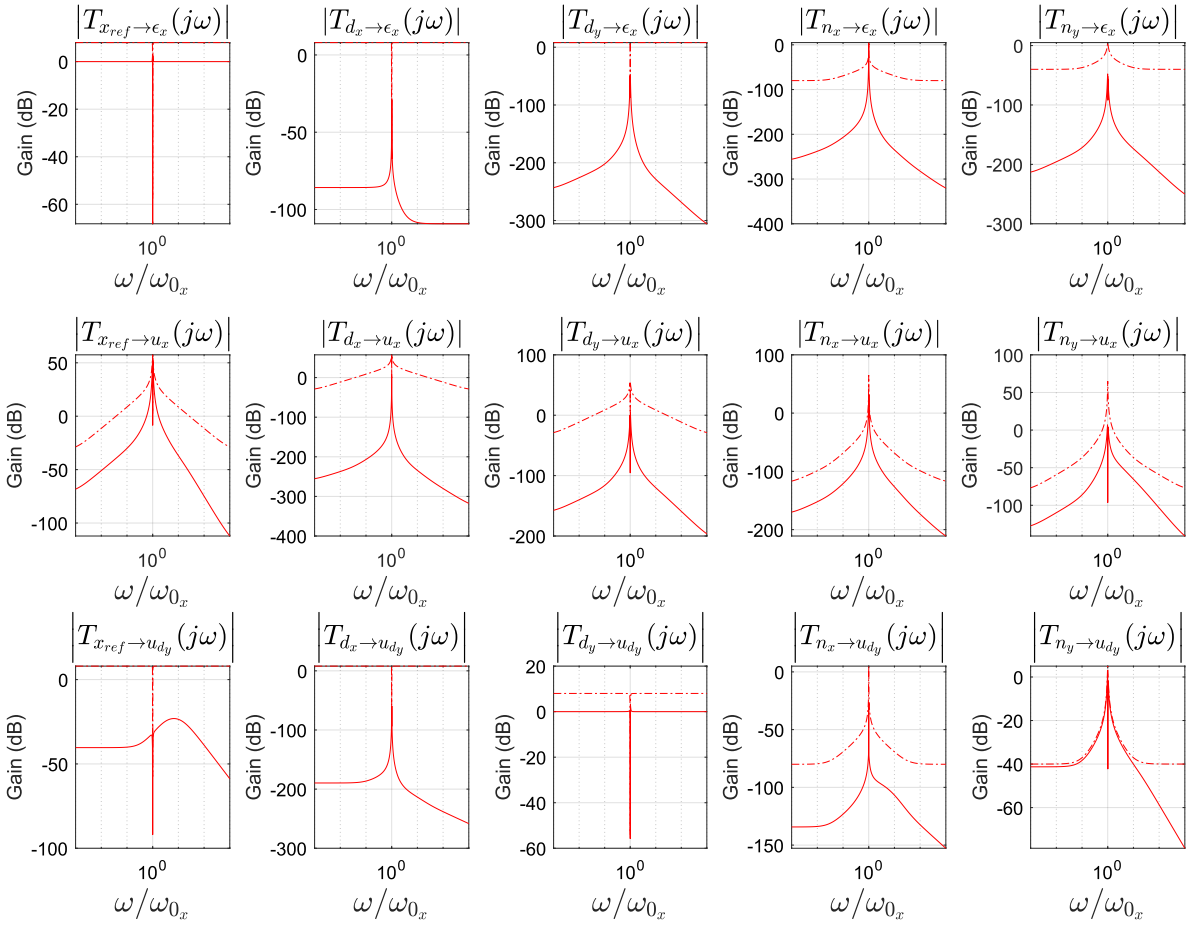

Fig. 8: Magnitudes of the closed-loop transfer functions (solid line) and upper bounds enforced by the weighting functions (dashed line).

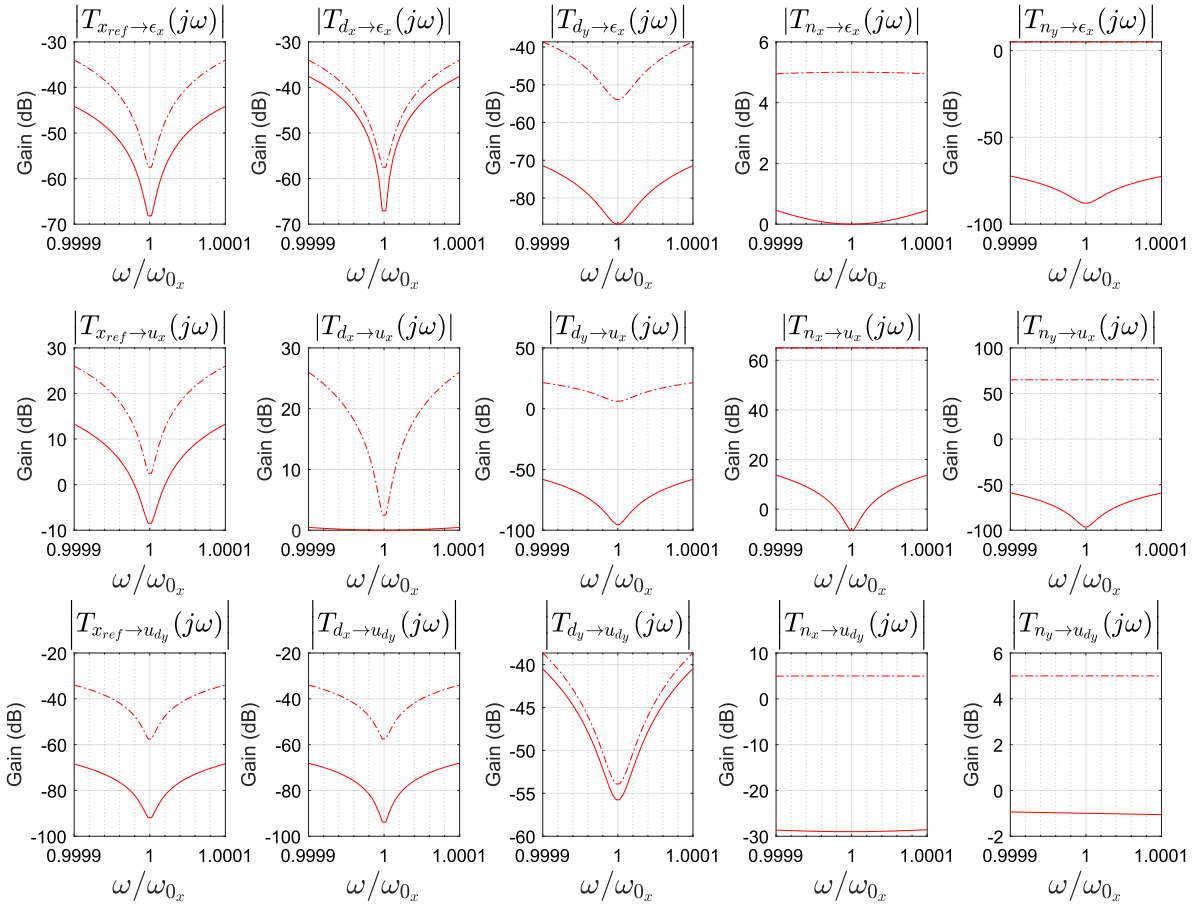

Fig. 9: Zoom around ω_{0_x} on the magnitudes of the closed-loop transfer functions (solid line) and upper bounds enforced by the weighting functions (dashed line).

REFERENCES

[1] F. Saggin, C. Pernin, A. Korniienko, G. Scorletti, and C. Le Blanc, "Digital Control of MEMS Gyroscopes: a Robust Approach," in *IEEE International Symposium on Inertial Sensors and Systems (INERTIAL)*. (to be published), 2021.

[2] K. Colin, F. Saggin, C. Le Blanc, X. Bombois, A. Korniienko, and G. Scorletti, "Identification-Based Approach for Electrical Coupling Compensation in a MEMS Gyroscope," in *IEEE International Symposium on Inertial Sensors and Systems (INERTIAL)*. IEEE, apr 2019, pp. 1–4. [Online]. Available: https://hal.archives-ouvertes.fr/hal-02174925

[3] K. Colin, "Data informativity for the prediction error identification of MIMO systems : identification of a MEMS gyroscope," Theses, Université de Lyon, Sep. 2020. [Online]. Available: https://tel.archives-ouvertes.fr/tel-03114994

[4] S. Skogestad and I. Postlethwaite, *Multivariable feedback control - analisys and design*, 2nd ed. John Wiley & Sons, 2001.

[5] G. Scorletti and V. Fromion, *Automatique fréquentielle avancée*, 2009. [Online]. Available: https://cel.archives-ouvertes.fr/cel-00423848v2

[6] G. Balas, R. Chiang, A. Packard, and M. Safonov, "The robust control toolbox of matlab," MathWork, Tech. Rep., 2020. [Online]. Available: https://fr.mathworks.com/help/pdf_doc/robust/index.html